Description of Transport Codes for Space Radiation Shielding

Myung-Hee Y. Kim[1], John W. Wilson[2], and Francis A. Cucinotta[3]

[1]Division of Space Life Sciences, Universities Space Research Association, Houston, TX 77058

[2]Distinguished Research Associates, NASA Langley Research Center, Hampton, VA 23681

[3]Space Radiation Program, NASA Johnson Space Center, Houston, TX 77058

NCRP 2011 Annual Meeting

Scientific and Policy Challenges of Particle Radiations in Medical Therapy and Space Missions

March 7-8, 2011

Introduction

- Radiation transport codes, when combined with Risk Projection models, are main tool for shielding study and design.
- Approaches to assess the accuracy of Transport Codes:
  - Ground-based studies with defined beams and material layouts
  - Inter-comparison of transport code results for matched boundary conditions
  - Comparisons to flight measurements
- NASA's HZETRN/QMSFRG code has a very high degree of congruence for each of these criteria.

Components of Space Radiation Shield Design

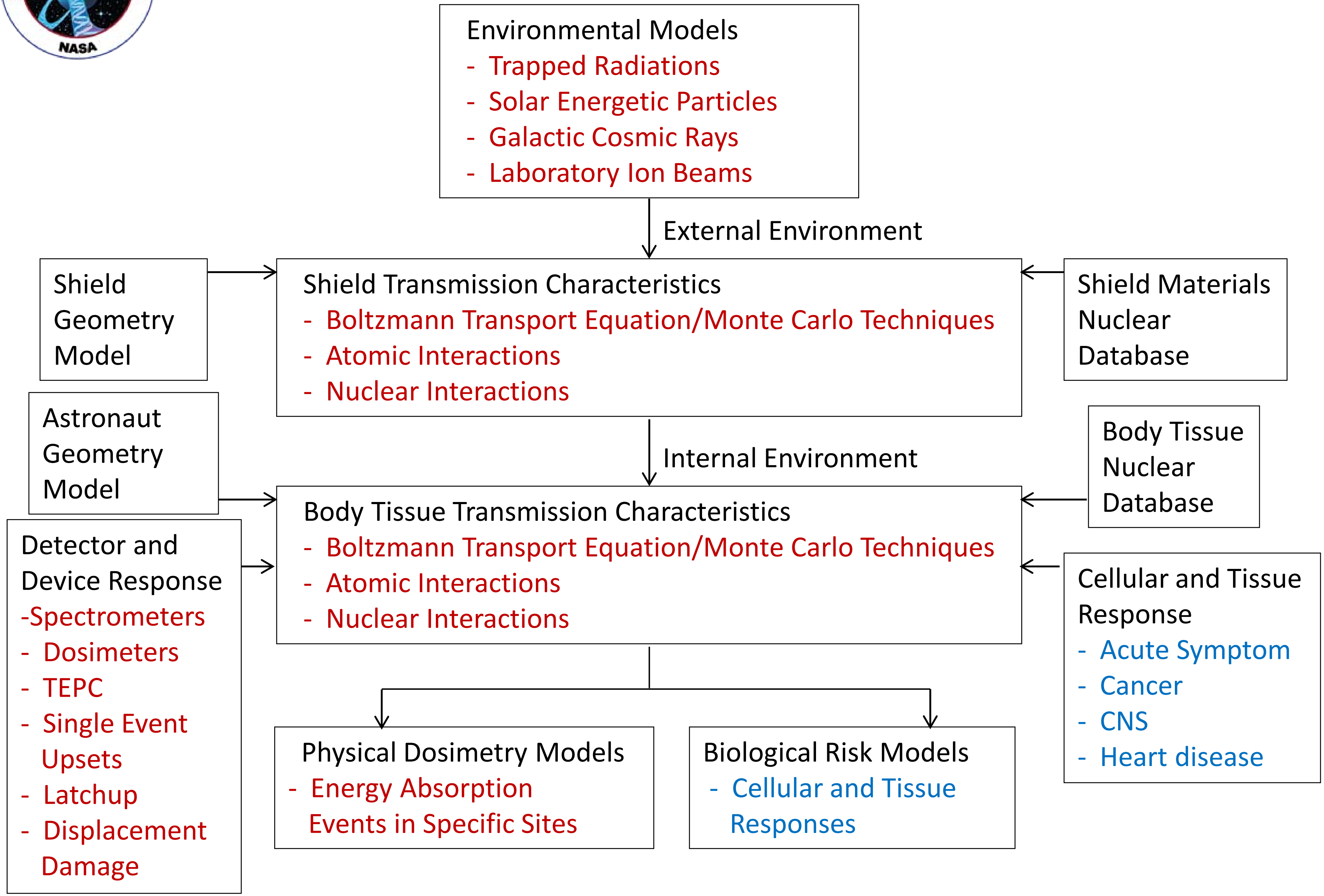

NSRL for Biophysics Applications

Approximate Composition

$N_{101.7}O_{33.1}Al_{36}$

Density: 0.00194 g/cm^3

Thickness: 1.2166 g/cm^2

N: 2.09 10^{22} atoms/g

O: 6.81 10^{21} atoms/g

Al: 7.41 10^{21} atoms/g

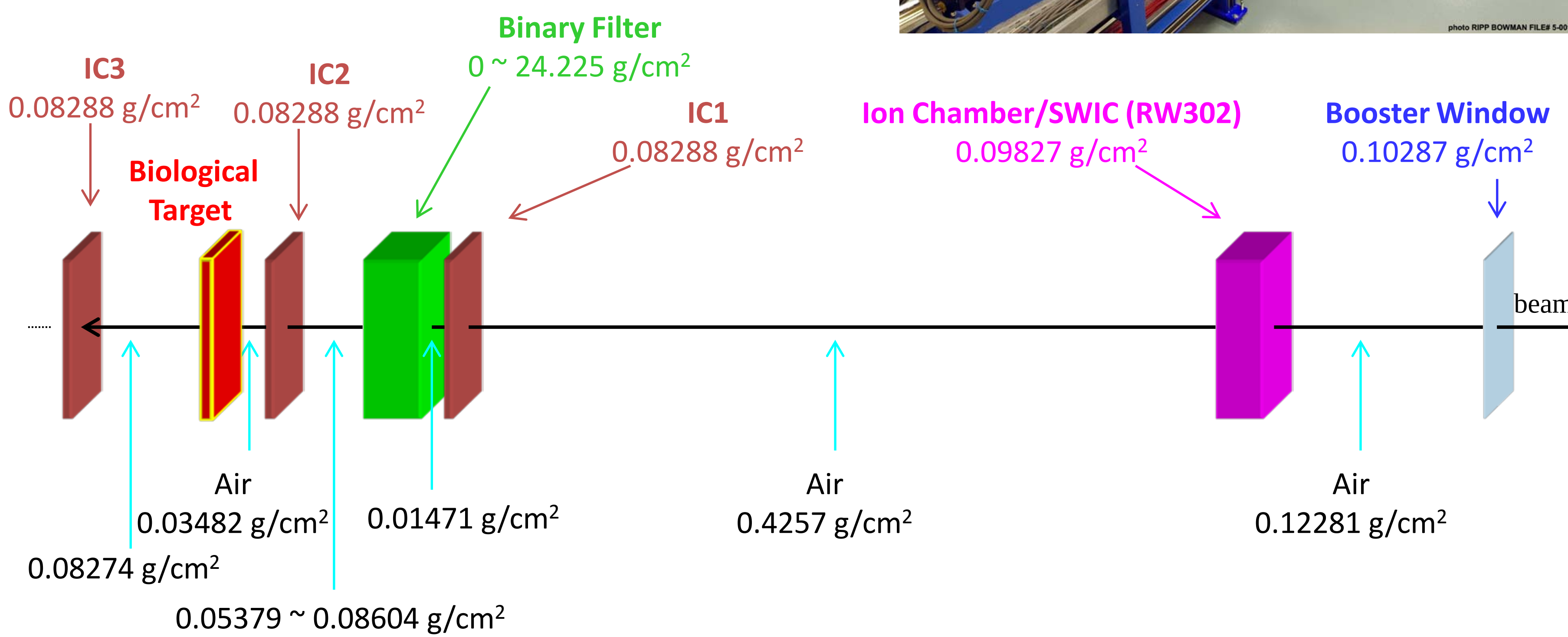

Heavy Ion Reactions

Abrasion=projectile-target overlap
(n, p, and cluster knock-out)
Ablation = pre-fragment decay
(n, p, d, t, h, alphas de-excitation)
Coalescence = p and n knockout
form bound states in couple phase
space

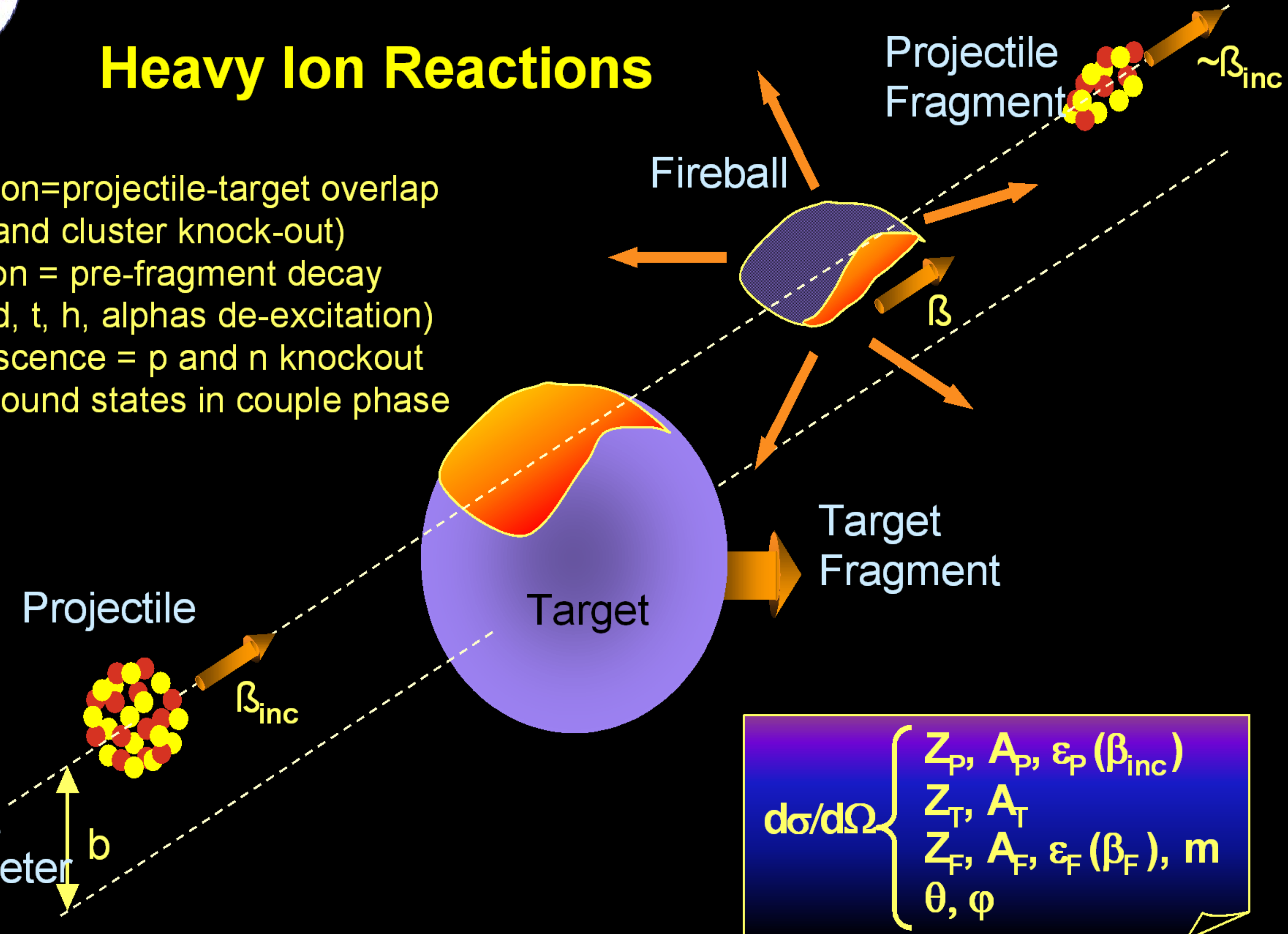

Fragmentation Cross Sections: Comparison of QMSFRG to Si and Fe Beams

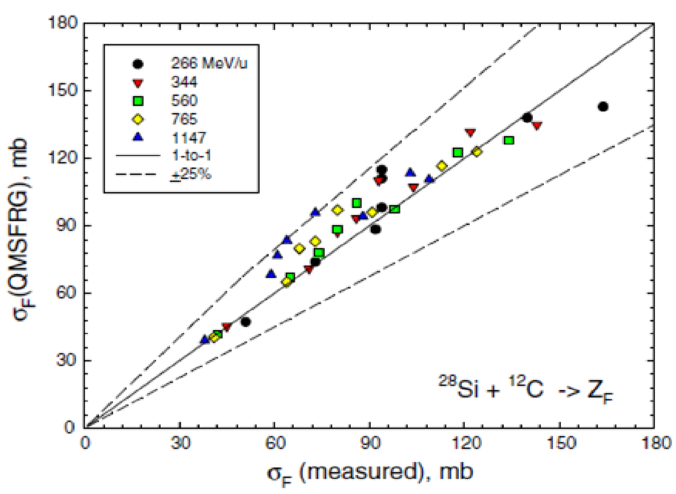

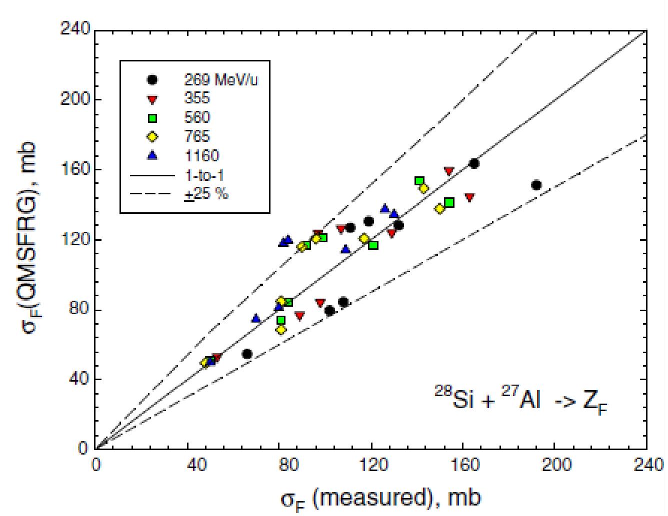

0.65 GeV/u

1.05 GeV/u

1.6 GeV/u

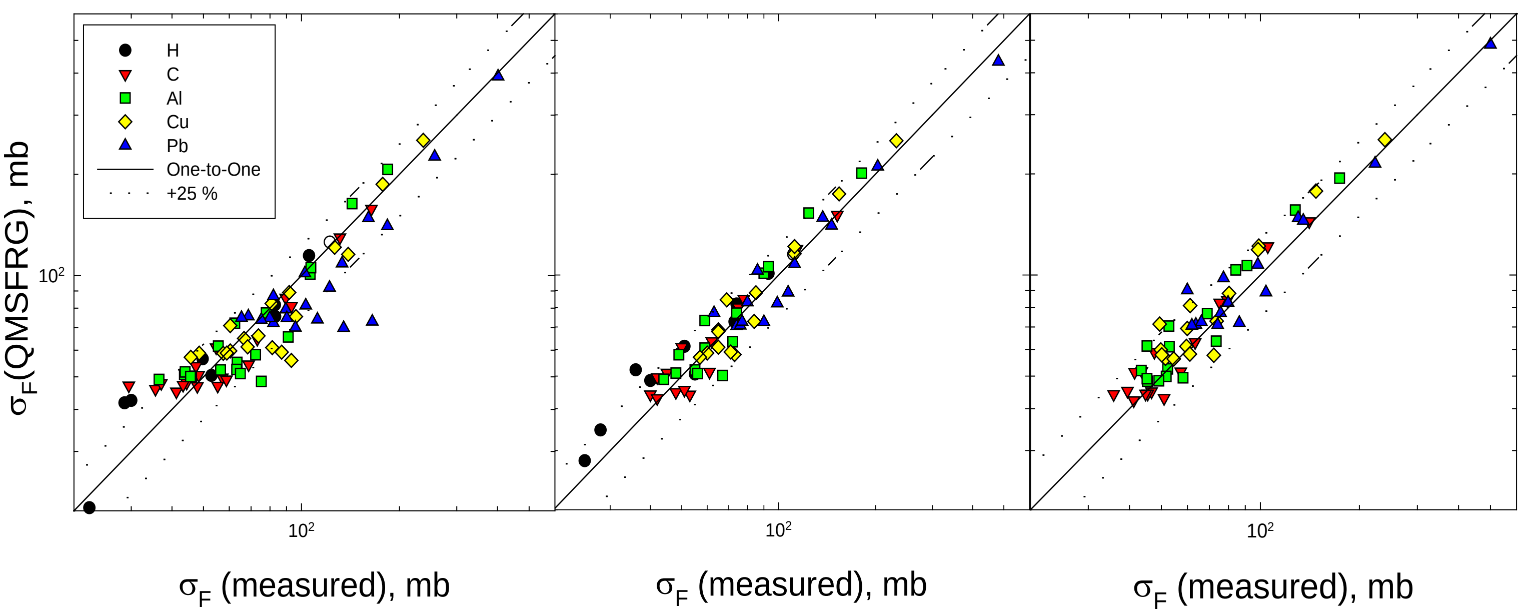

NSRL Bragg Curve Comparison to GCR Event-based Risk Model (GERM)

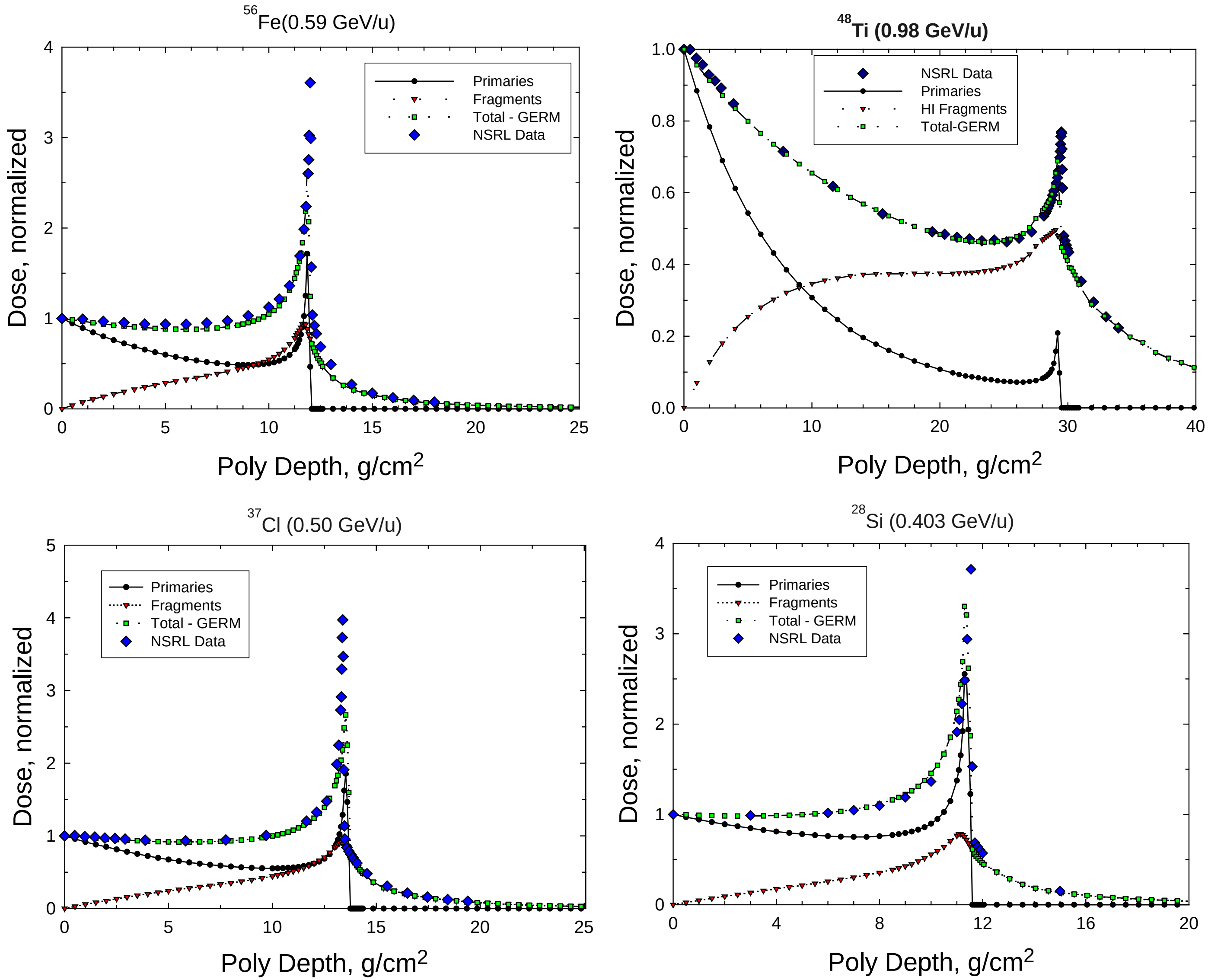

Cucinotta FA et al., Radiat Prot Dosimetry, 2011

Thick Target Comparison with NASA's GERMCode* and GRNTRN Code*

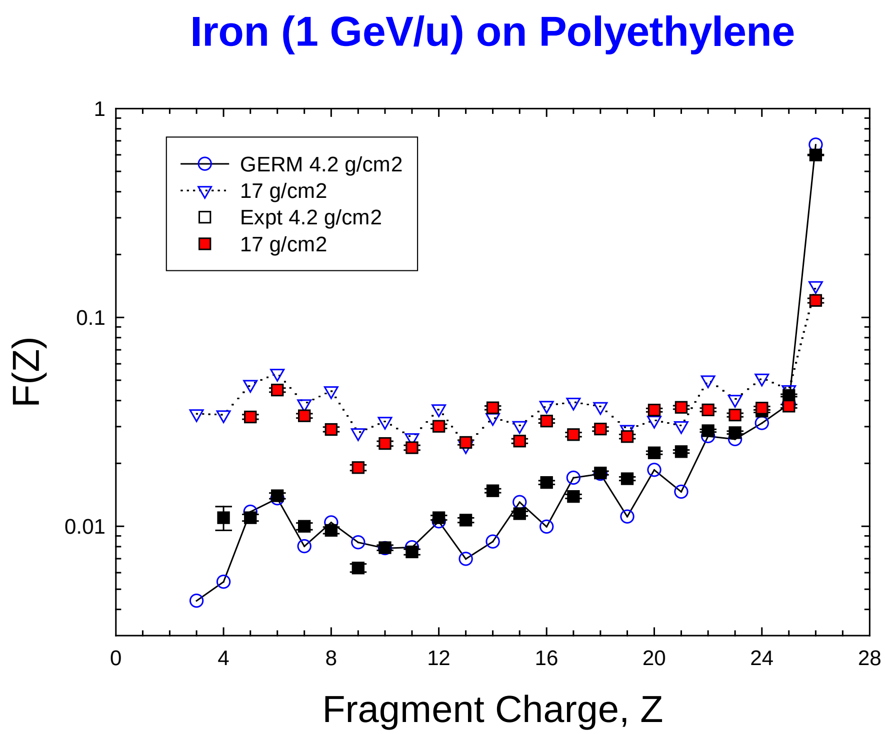

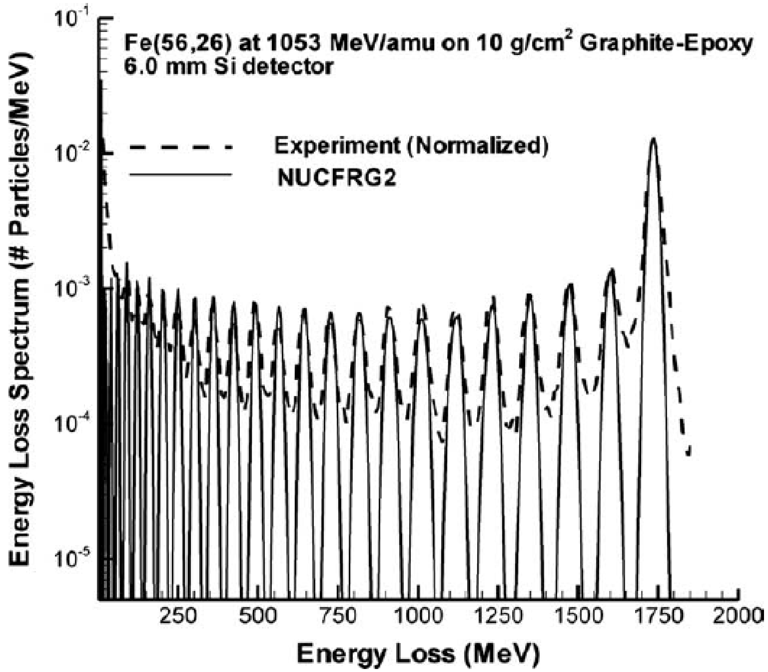

*HZETRN uses identical Nuclear Cross Sections and Atomic Data

Space Weather Prediction Center, NWS, NOAA

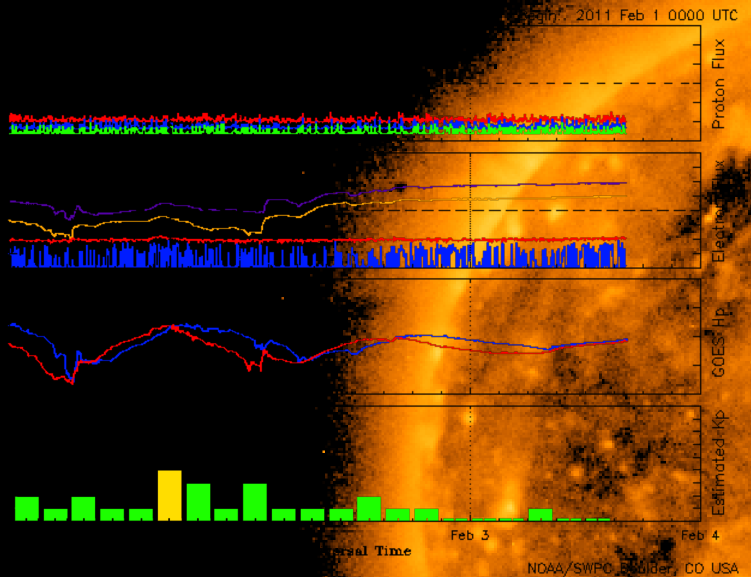

Satellite Environment

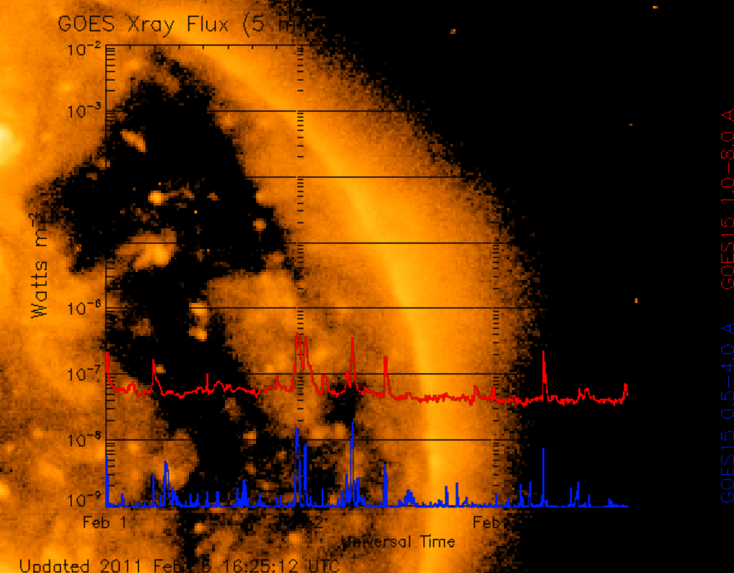

GOES Solar X-ray Flux

NOAA Scales Activity

Range 1 (minor) to 5 (extreme)

NOAA Scale	Past 24 hours	Current
Geomagnetic Storms	none	none
Solar Radiation Storms	none	none
Radio Blackouts	none	none

Space Environmental Models
Fit to Proton Measurements for Continuous Spectrum

Functional Forms with Measurements

- Exponential in Rigidity or Energy: $\Phi(>R)=J_0 \exp(-R/R_0)$ or $\Phi(>E)=J_0 \exp(-E/E_0)$
- Sum of Two Exponentials : $\Phi(>E)=J_1 \exp(-E/E_1) + J_2 \exp(-E/E_2)$
- Weibull Function in Energy : $\Phi(>E)=J_0 \exp(-\kappa E^{\alpha})$

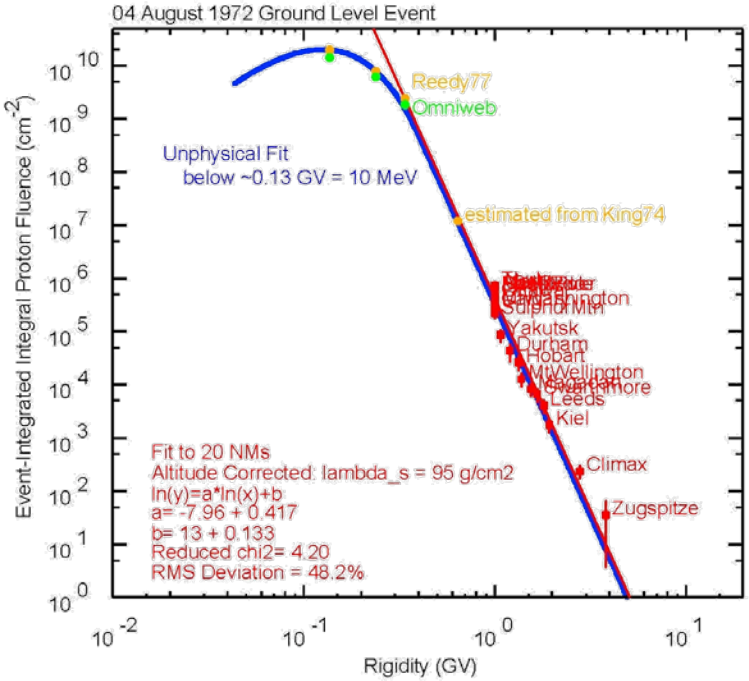

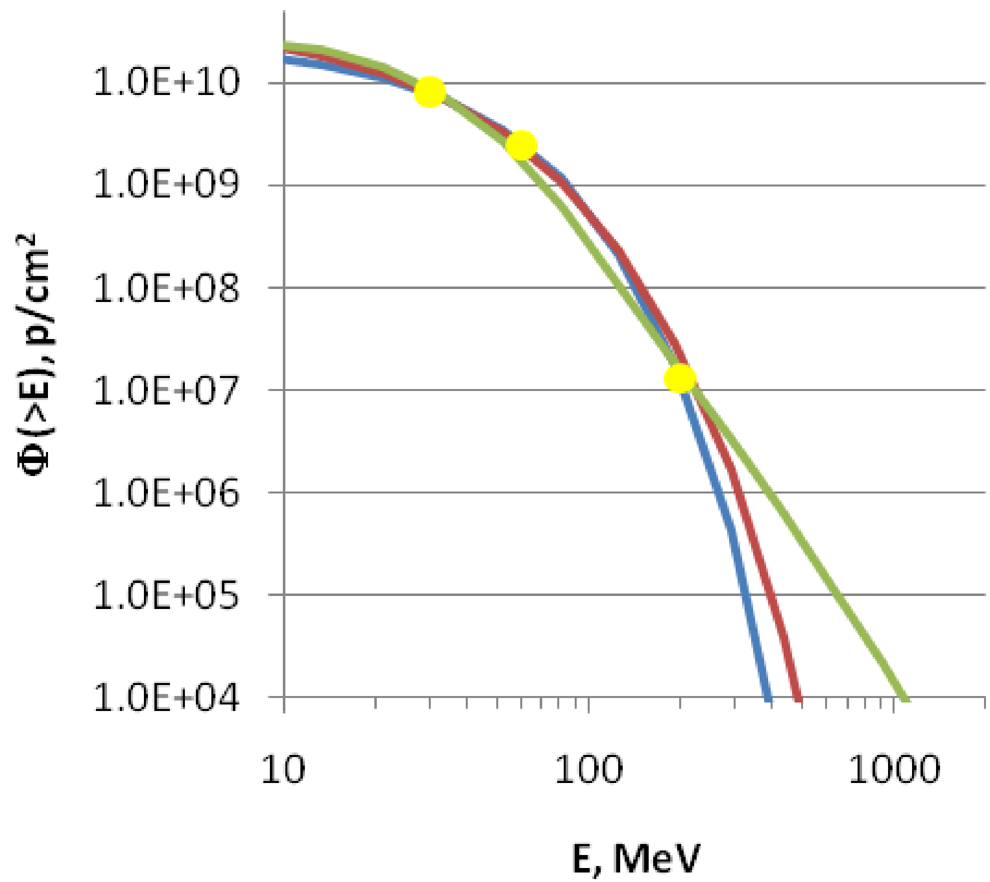

Band Function with 4 Parameters ($J_0, \gamma_1, \gamma_2, R_0$): Double Power Law in Rigidity

$$\Phi(>R) = J_0 R^{-\gamma_1} e^{-R/R_0} \quad \text{for } R \le (\gamma_2-\gamma_1)R_0$$

$$\Phi(>R) = J_0 R^{-\gamma_2} \left\{ \left[(\gamma_2-\gamma_1)R_0\right]^{(\gamma_2-\gamma_1)} e^{(\gamma_1-\gamma_2)} \right\} \quad \text{for } R \ge (\gamma_2-\gamma_1)R_0$$

Interplanetary Galactic Cosmic Ray Energy Spectra

Advanced Composition Explorer/Cosmic Ray Isotope Spectrometer

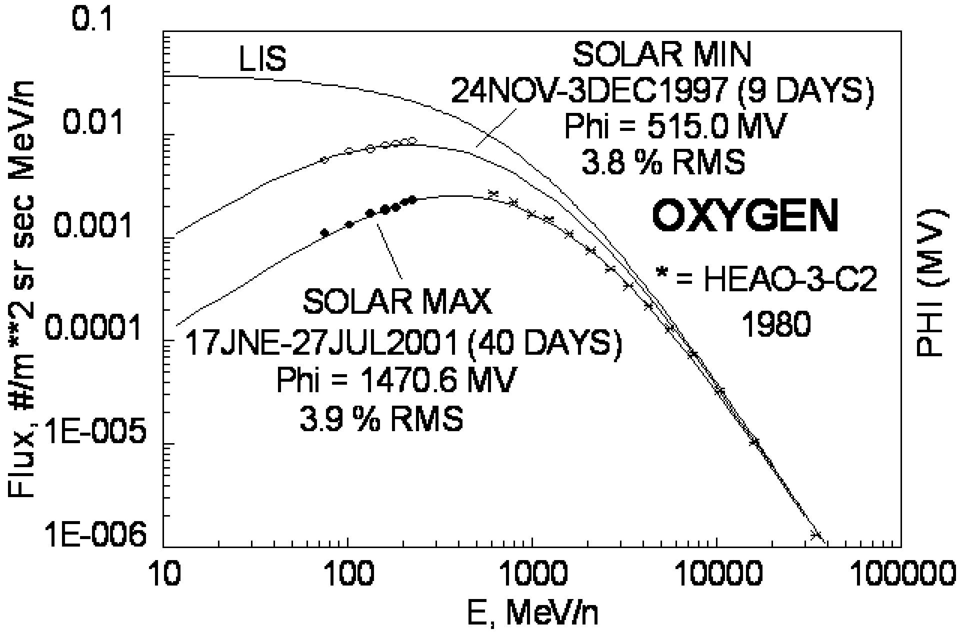

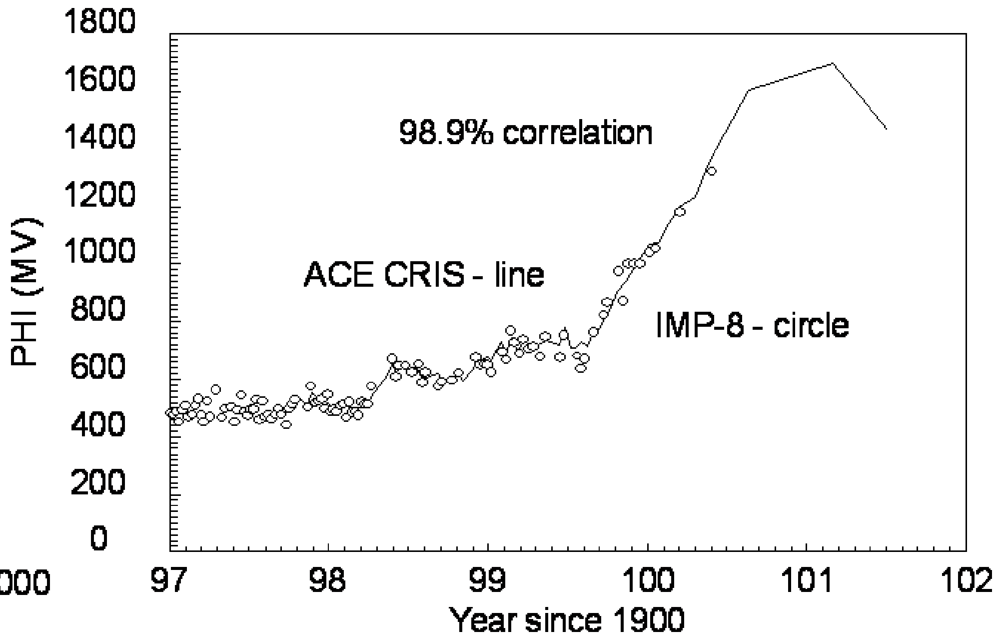

Badhwar-O'Neill Model fit of ACE CRIS oxygen energy spectra measurements near solar minimum and near solar maximum

Solar modulation parameter:
ACE CRIS oxygen measurements (line);
IMP-8 (Z>8) channel 7 measurements (○)

O'Neil PM, 2010

Geometry Models

Shield Geometry Model and Shielding Analysis by CAD

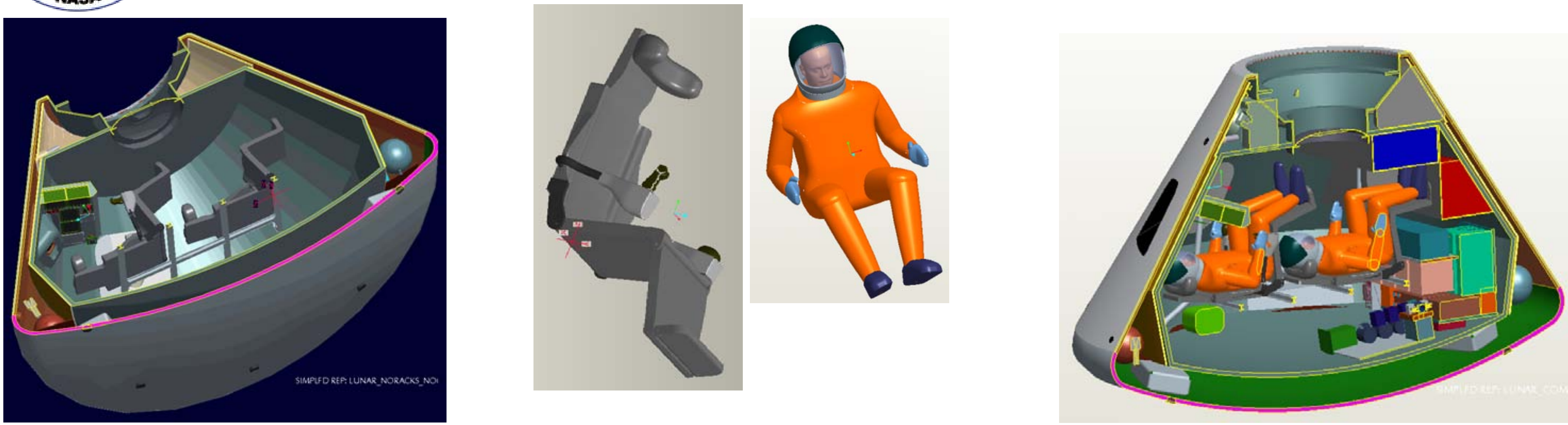

Structural Distribution Model for Layers of Spacecraft Using ProE™/Fishbowl

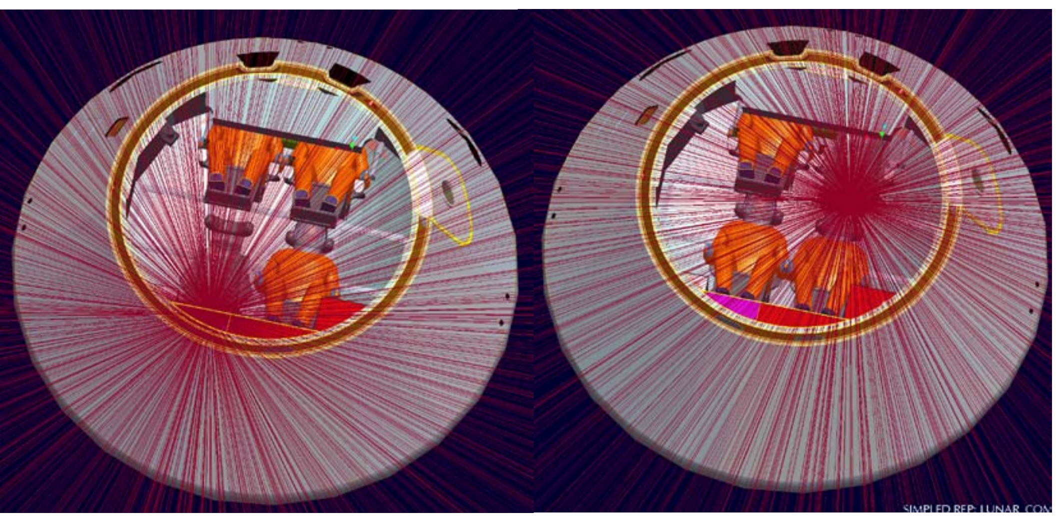

Ray Tracing inside Spacecraft

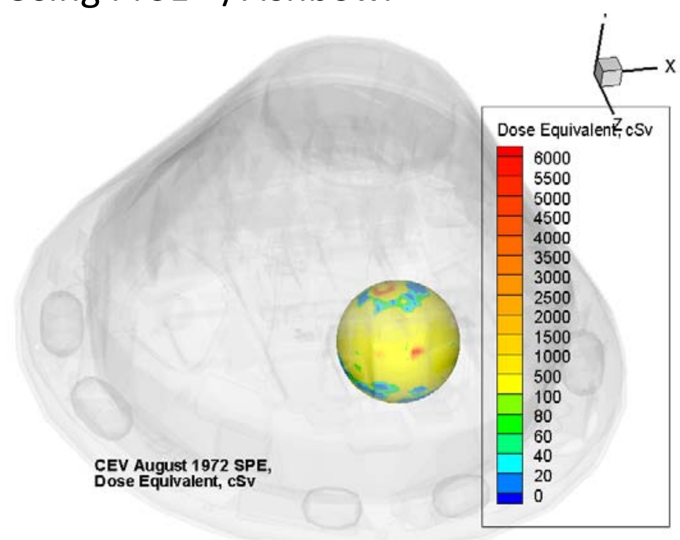

Color-coded Representation of Directional Shielding

Human Geometry Models and Active Marrow Distributions

Computerized Anatomical Male

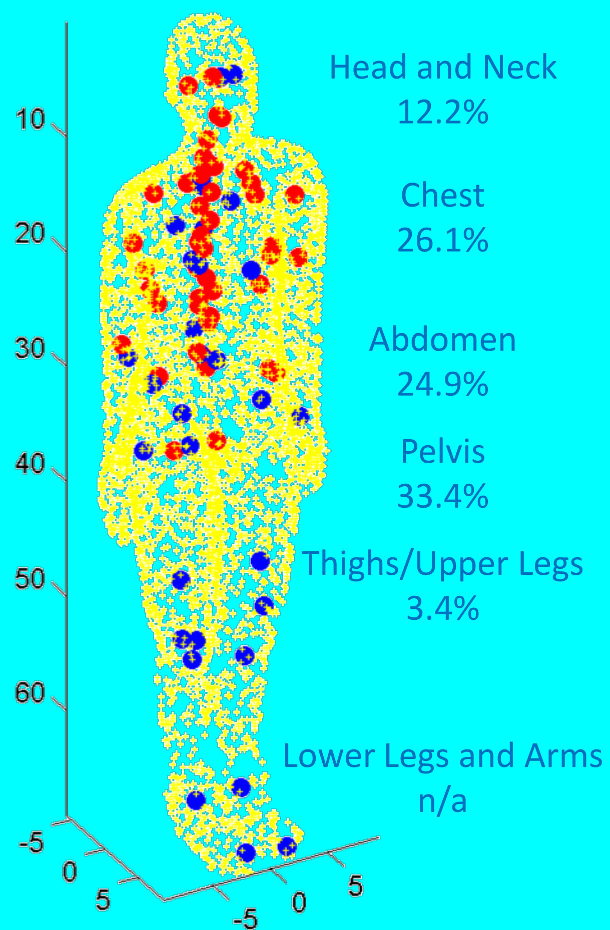

Male Adult voXel

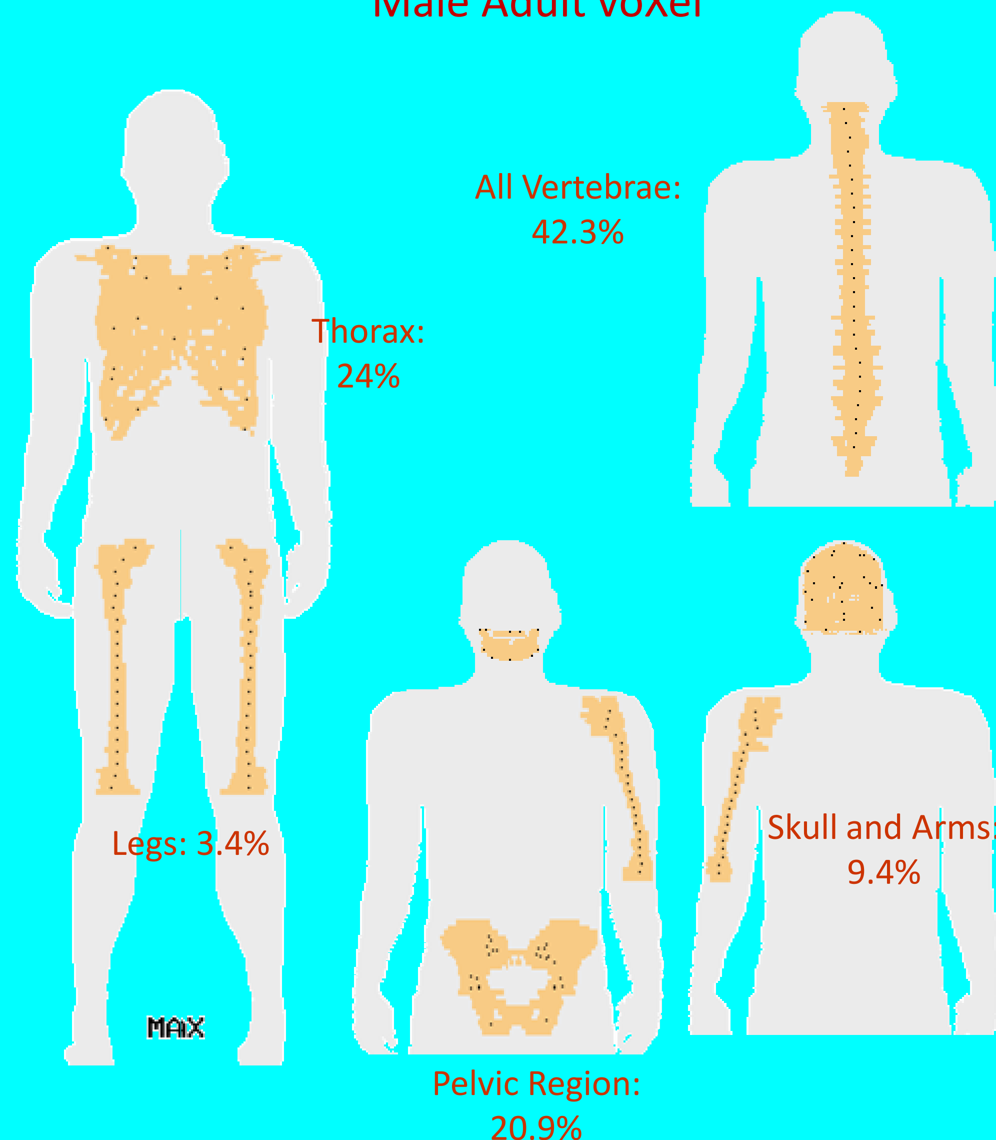

Inter-Comparisons of Transport Codes

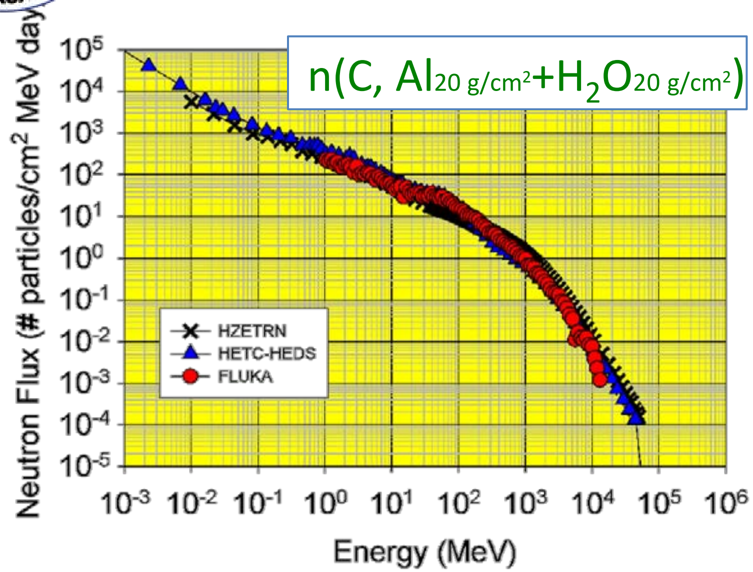

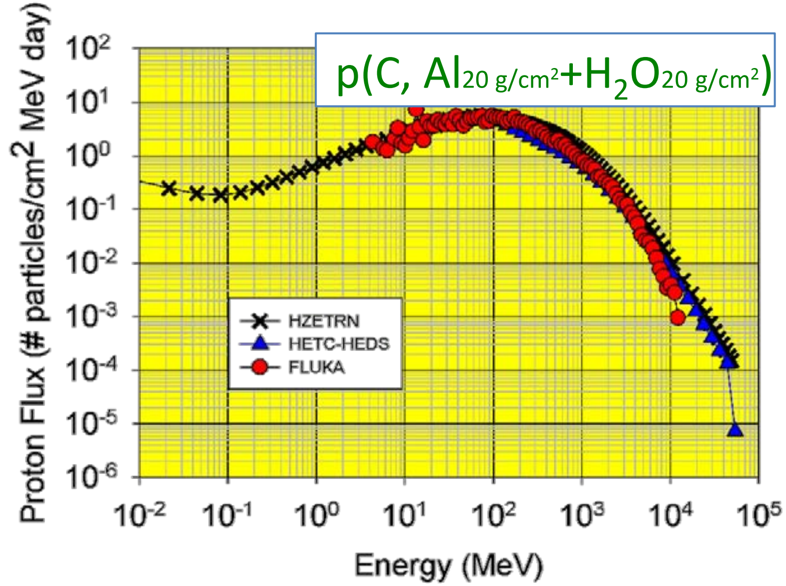

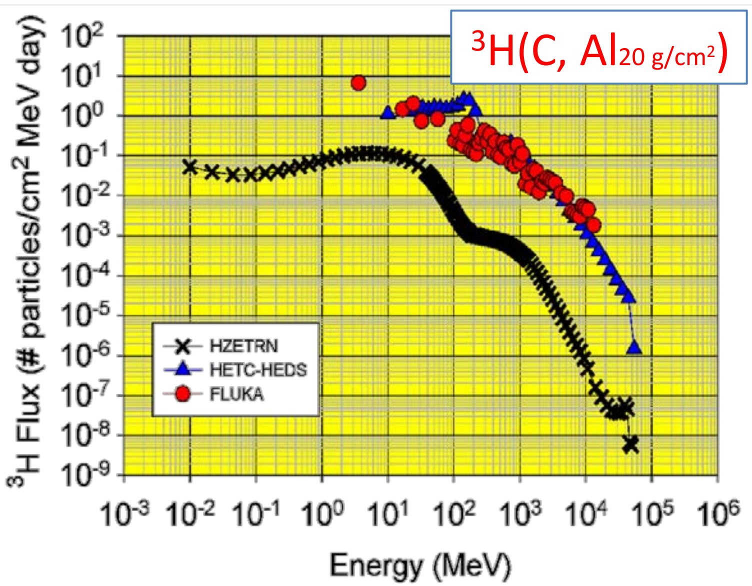

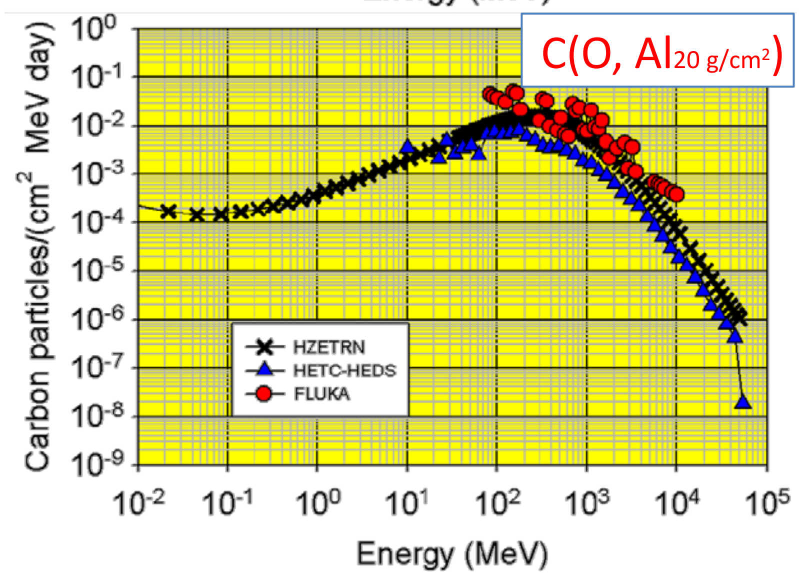

Heinbockel JH et al., NASA TP 2009-215560, 2009

Comparisons with Flight Measurements

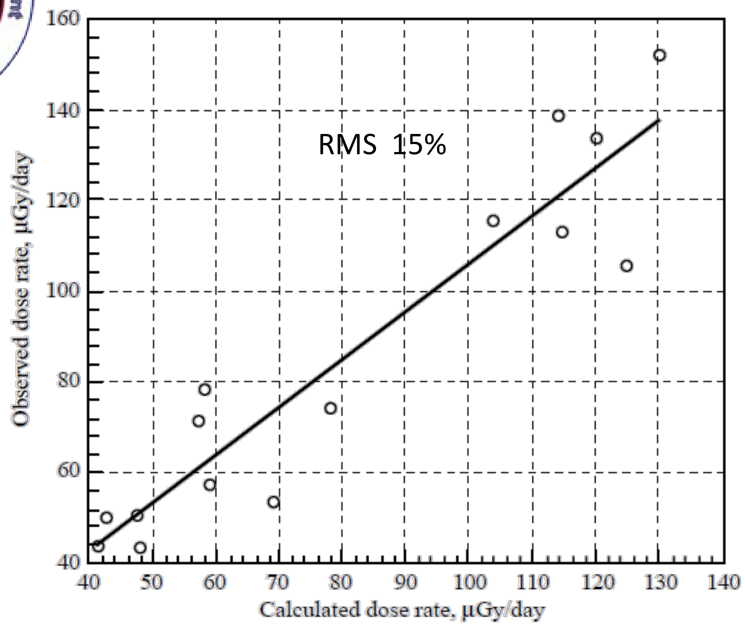

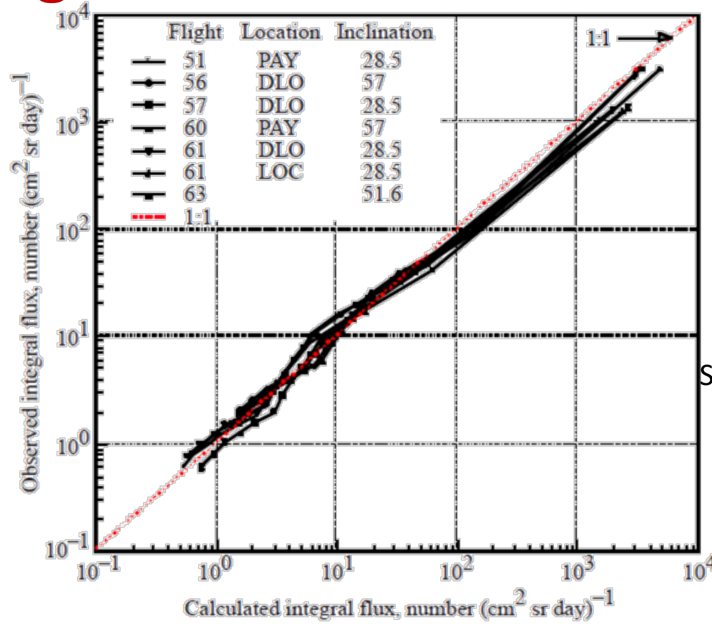

1.5-2.7X
Albedo protons
Albedo neutrons
Secondary neutron
Geomagnetic
tansmission
function

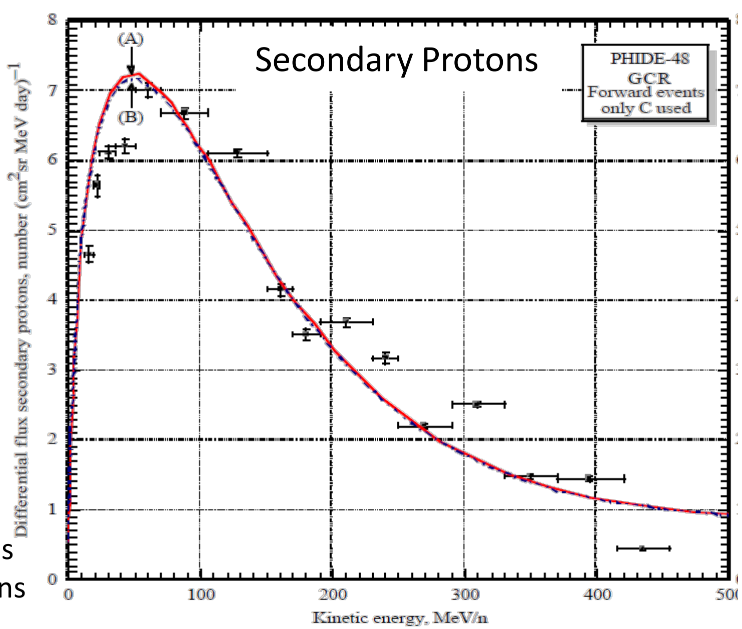

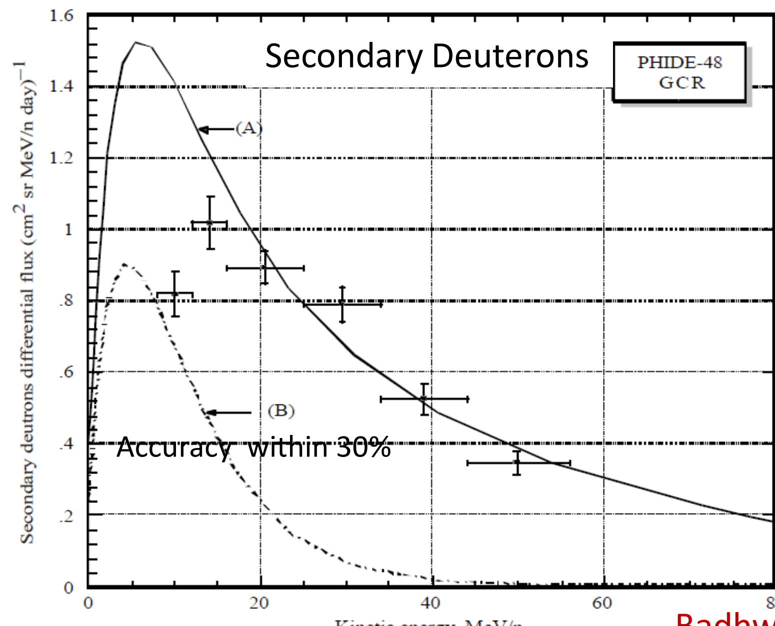

25%
Albedo protons
Secondary pions
Kaons

Badhwar GD, 1997

Evaluation of Detector Response
- TEPC Response for Trapped Protons on STS-89 -

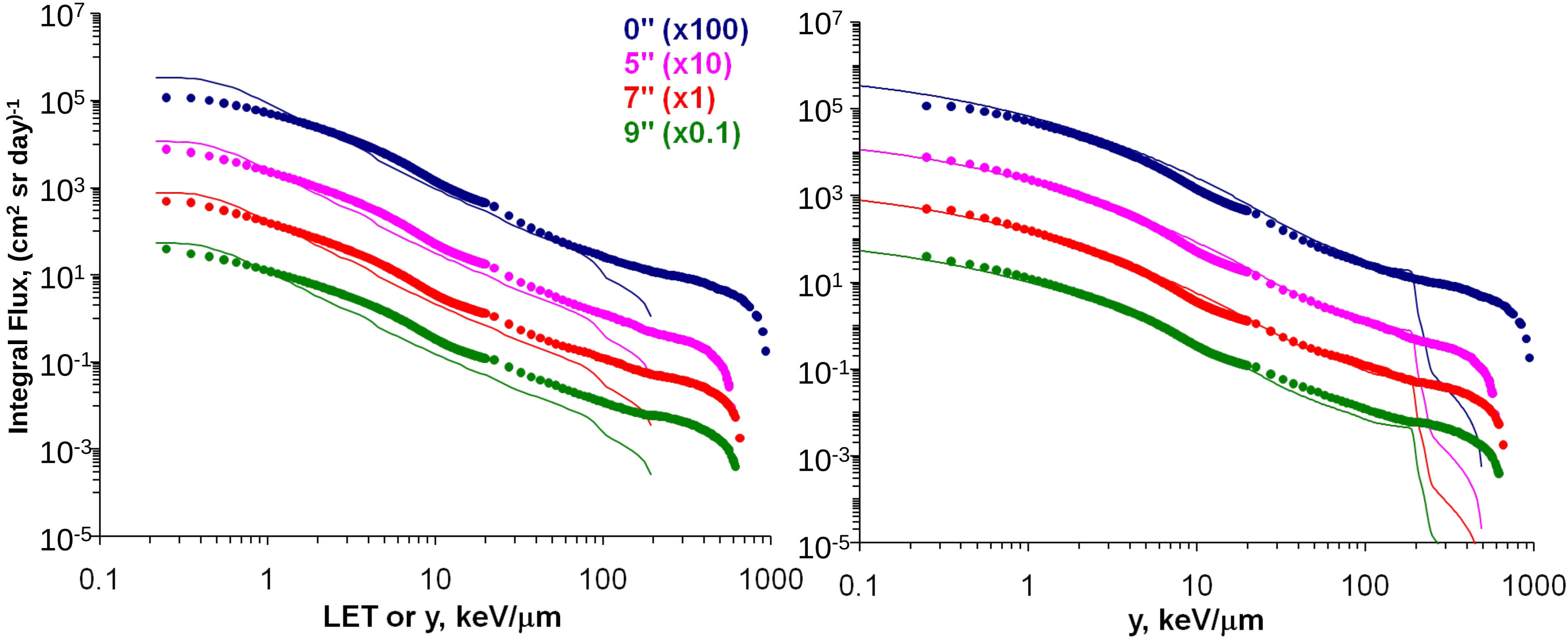

without TEPC response

with TEPC response

Phantom Torso Experiment (PTE) of ISS/STS
TLD Dose Contours of Brain Slice

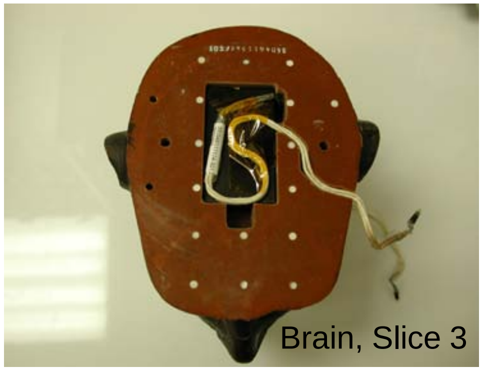

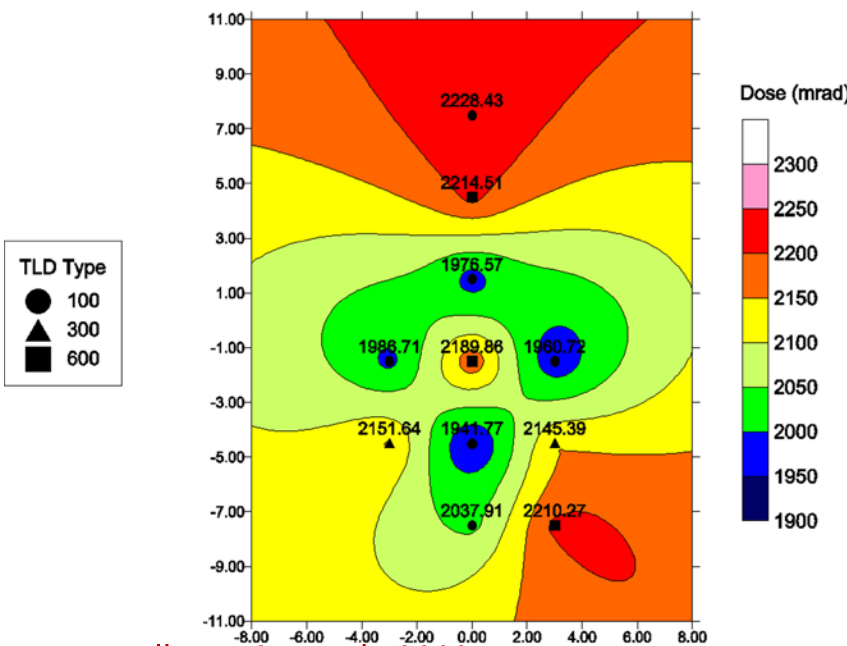

Badhwar GD et al., 2002

Organ Dose Equivalent using CR-39/TLD, mSv			
Tissue	Measured	HZETRN/QMSFRG	Difference (%)
Skin	4.5±0.05	4.7	4.4
Thyroid	4.0±0.21	4.0	0
Bone surface	5.2±0.22	4.0	-23.1
Esophagus	3.4±0.49	3.7	8.8
Lung	4.4±0.76	3.8	-13.6
Stomach	4.3±0.94	3.6	-16.3
Liver	4.0±0.51	3.7	-7.5
Bone marrow	3.4±0.40	3.9	14.7
Colon	3.6±0.42	3.9	8.3
Bladder	3.6±0.24	3.5	-2.8
Gonad	4.7±0.71	3.9	-17.0
Chest	4.5±0.11	4.5	0
Remainder	4.0±0.57	4.0	0
Effective dose	4.1±0.22	3.9	-4.9

Yasuda et al., 2002

Active Dosimetry Data, mGy/d							
Organ	Trapped		GCR		Total		Difference
	Expt	Model	Expt	Model	Expt	Model	(%)
Brain	0.051	0.066	0.076	0.077	0.127	0.143	13.3
Thyroid	0.062	0.072	0.074	0.077	0.136	0.148	9.4
Heart	0.054	0.061	0.075	0.076	0.129	0.137	6.7
Stomach	0.050	0.057	0.076	0.077	0.126	0.133	5.5
Colon	0.055	0.056	0.073	0.076	0.128	0.131	2.5

Cucinotta FA et al., 2008

Predictions for Mars Mission

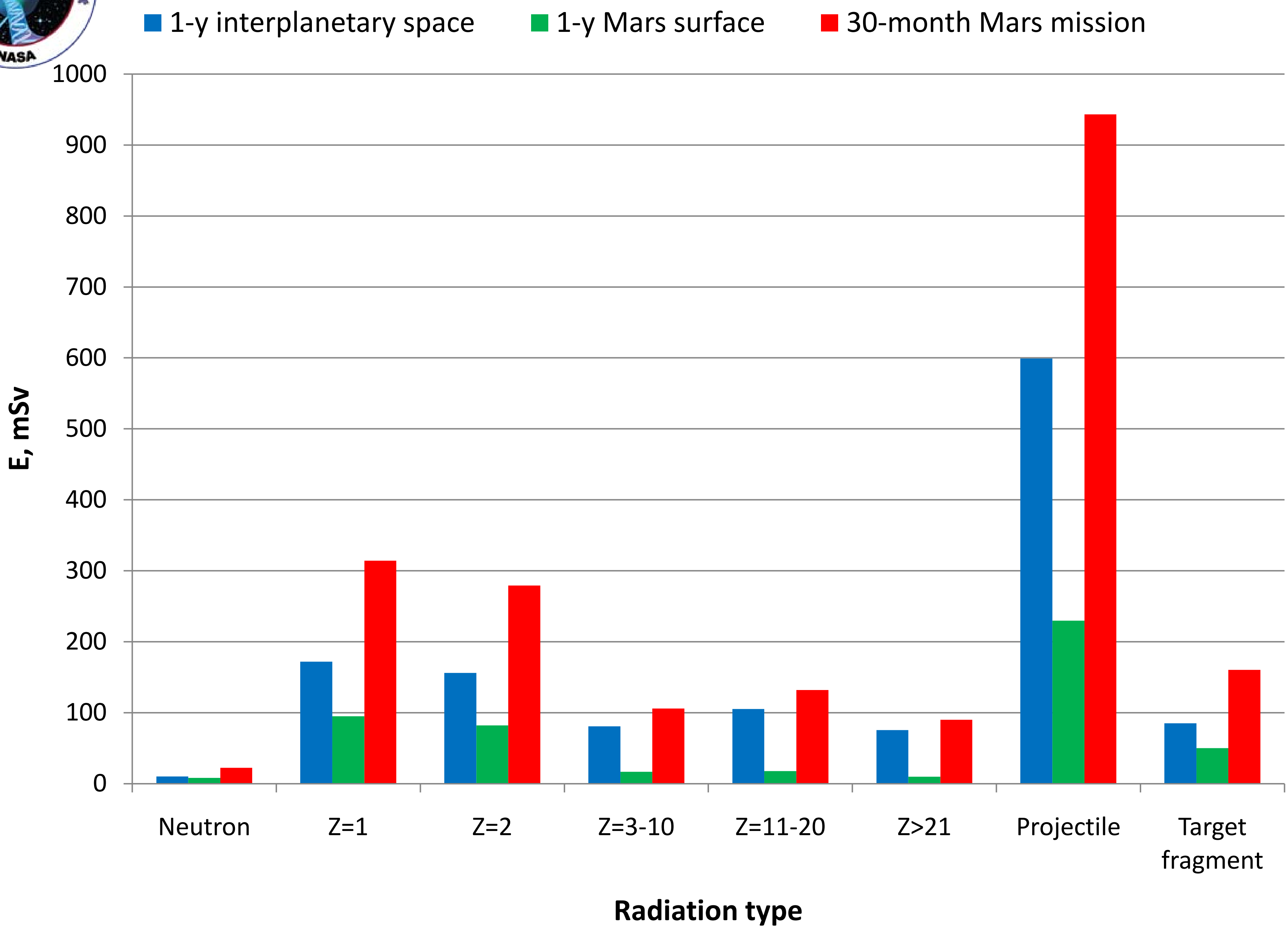

Annual Effective Dose for Male

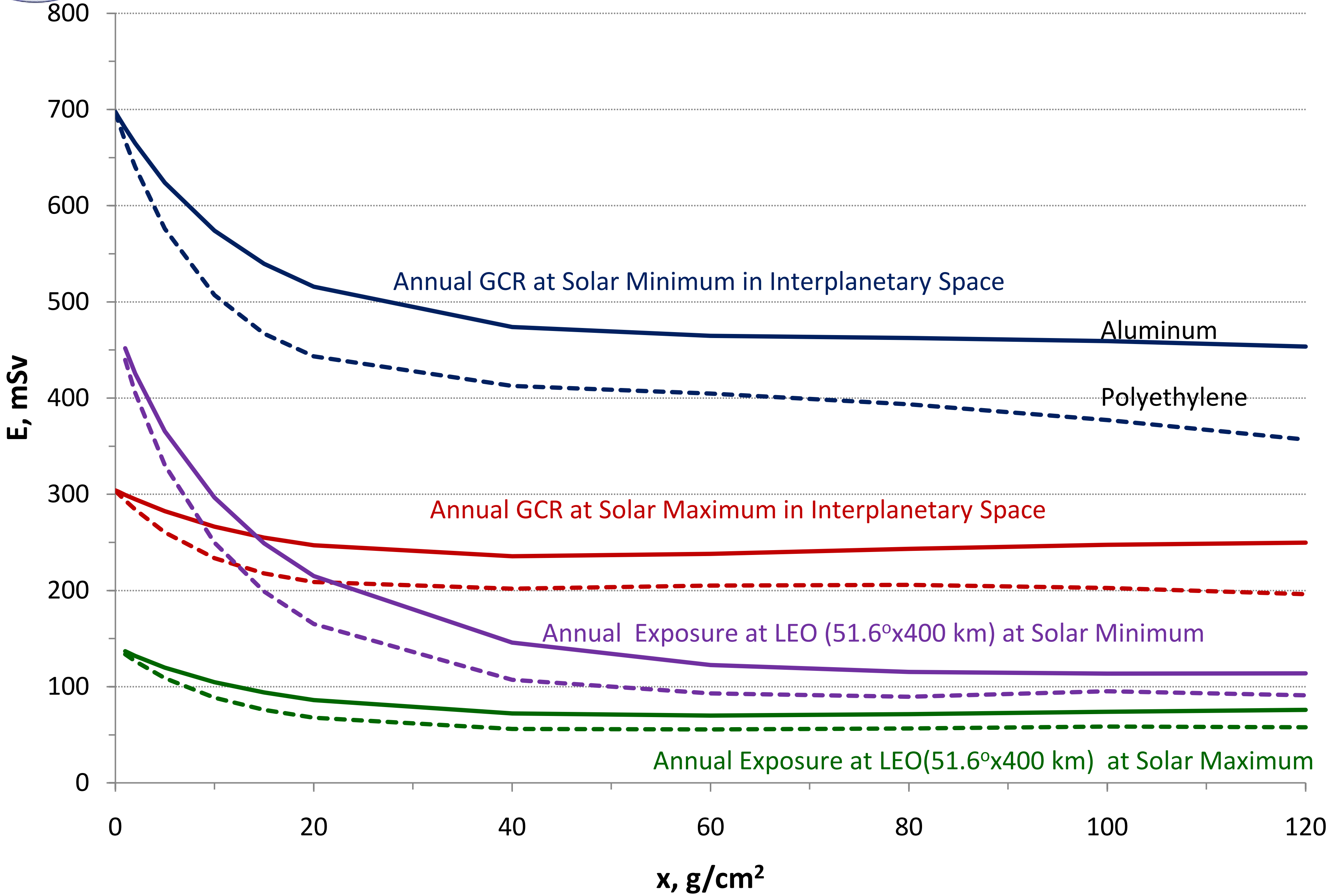

Model-based Prediction of SPE Occurrence

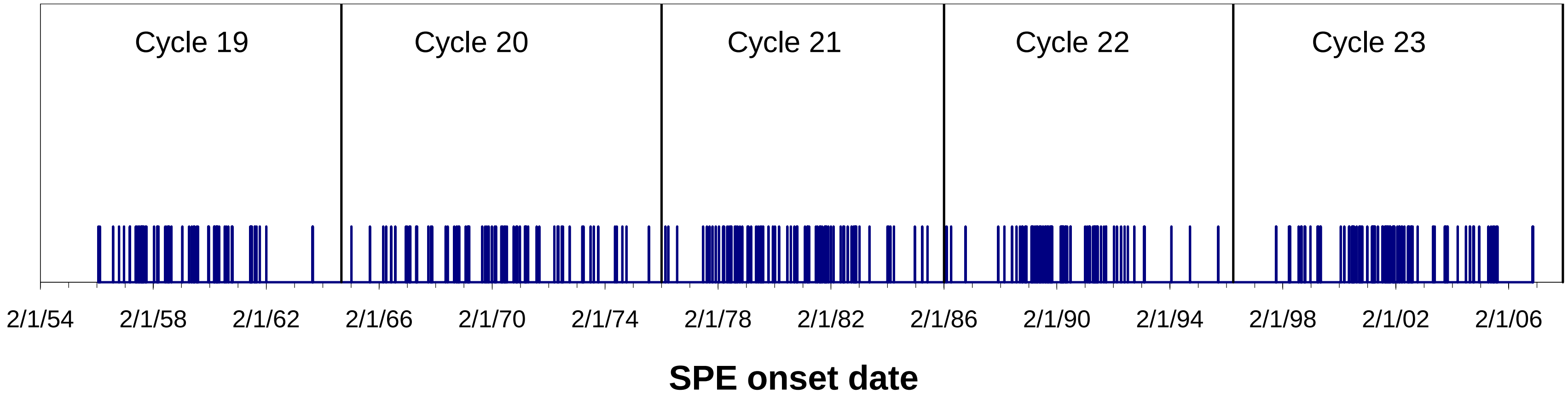

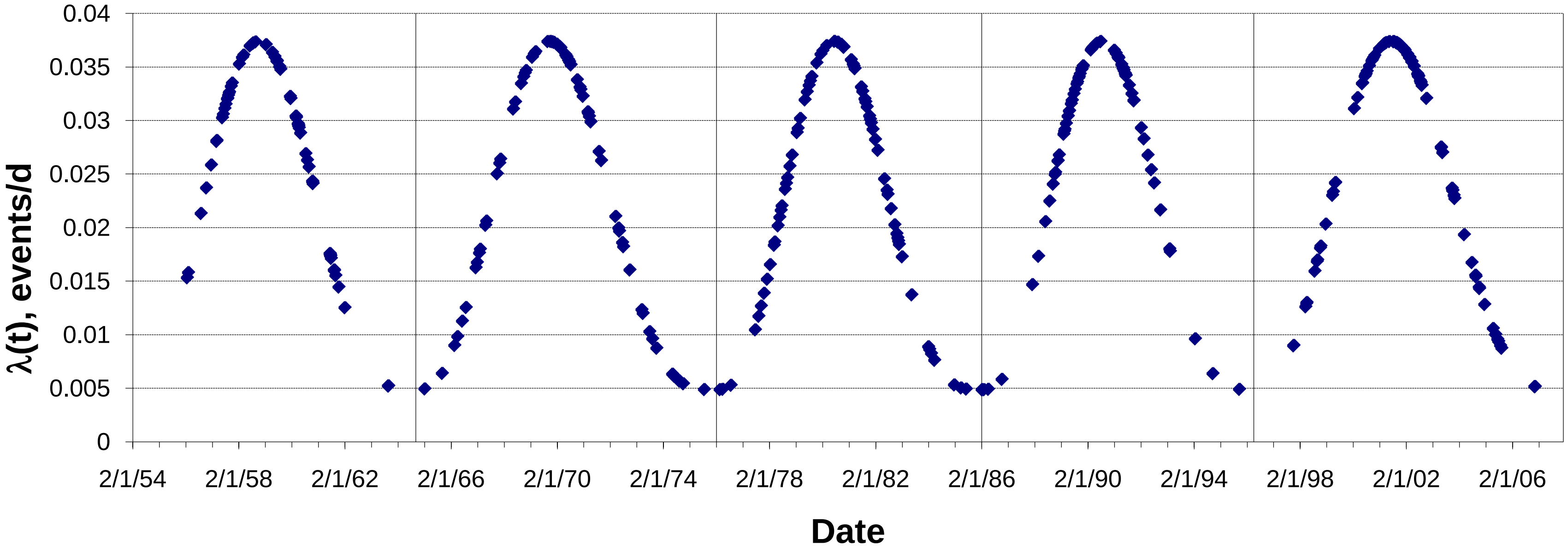

Model-based Prediction of SPE Fluence

Propensity of SPEs: Hazard Function of Offset β Distribution Density Function

$$\lambda(t) = \frac{\lambda_0}{4000} + \frac{K}{4000}\frac{\Gamma(p+q)}{\Gamma(p)\Gamma(q)}\left(\frac{t}{4000}\right)^{p-1}\left(1-\frac{t}{4000}\right)^{q-1} \quad (0 \le t \le 4000)$$

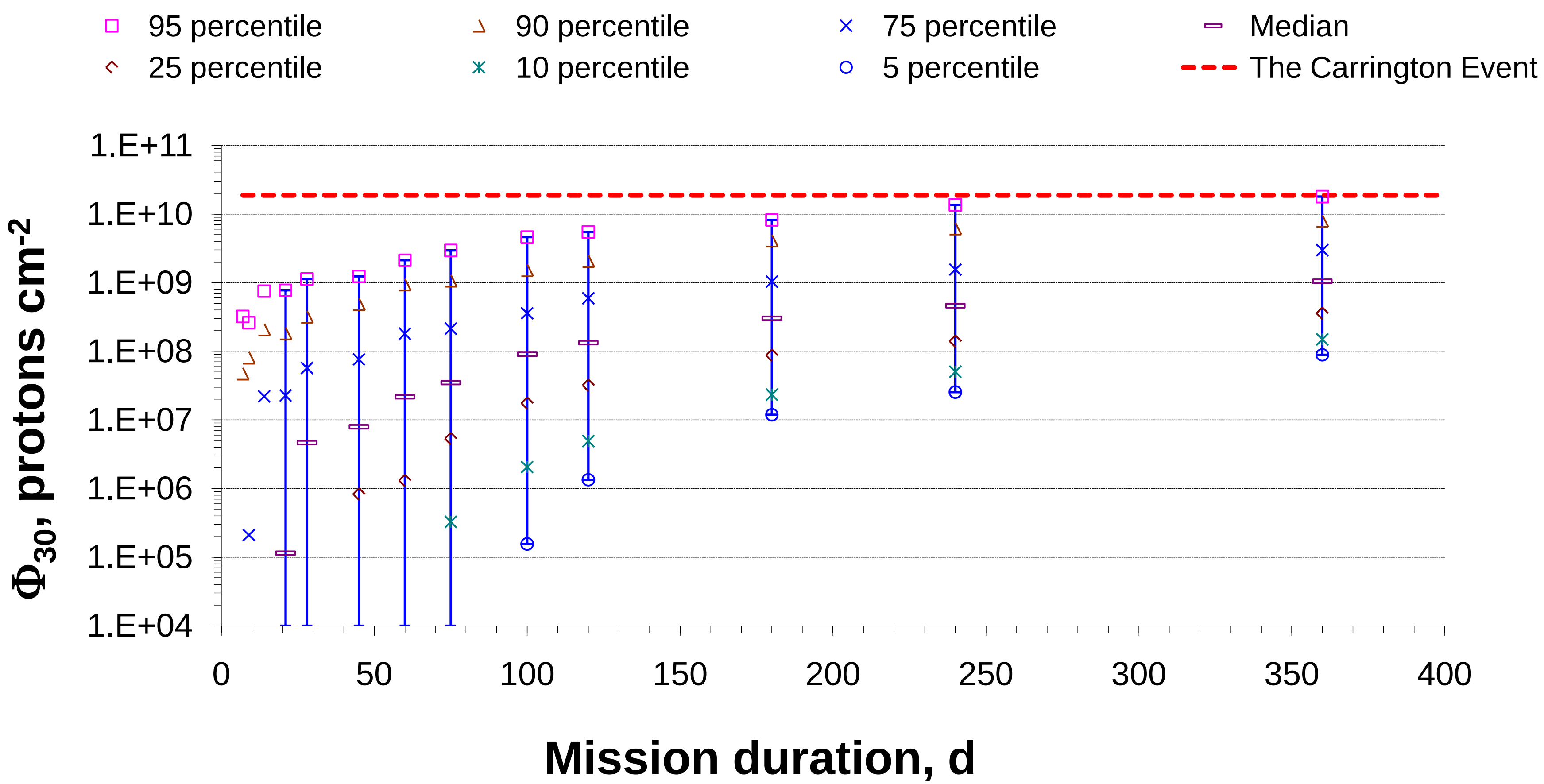

Effective dose on Mars Surface with MOLA Topography

Altitude, km	T, °C	p, kPa	Atmospheric shielding thickness, g/cm^2	
			Low density model	High density model
8.0	-41.16	0.34	0.14	0.19
4.0	-34.99	0.49	6.73	9.25
2.0	-33.00	0.58	10.97	15.08
0.0	-31.00	0.7	16.00	22.00
-2.0	-29.00	0.84	19.04	26.17
-4.0	-27.01	1.00	22.64	31.13
-8.0	-23.02	1.44	32.00	44.00

August 1972 SPE

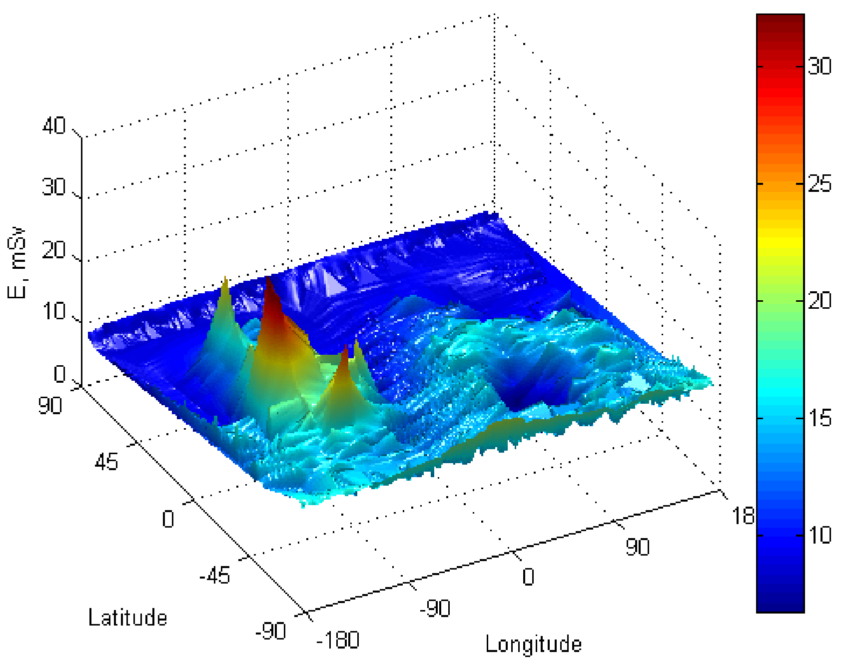

Annual GCR at Solar Minimum

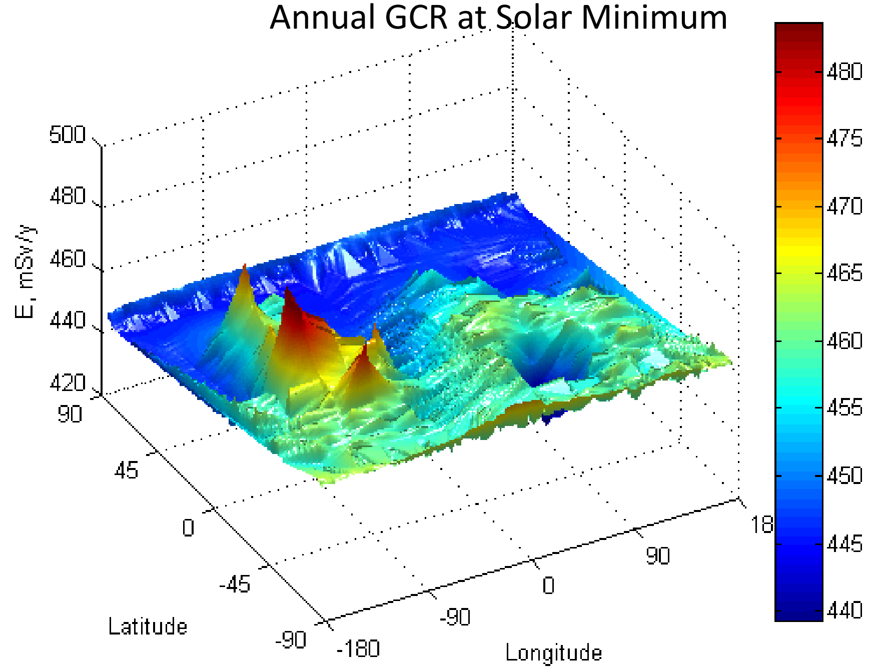

Conclusion

- Highly accurate descriptions of space environment models are available:
  - Inter-stellar GCR composition accuracy : ~5% for abundant elements (oxygen, carbon, and iron); less than 10% for all major GCR components; and solar modulation parameters with the 98.9% correlation in various spacecraft measurements.
  - Probabilistic SPE occurrence model as a tool for managing the risk.
    - Comprehensive catalogue of GLE fluences and spectra assembled for shielding design application using satellites and NM spectra;
- Radiation transport codes have been validated extensively:
  - QMSFRG model agrees for absorption σ-section within +5% and elemental fragment σ-section $\pm$25%.
  - Good agreement found from inter-comparisons of transport codes.
  - Comparison of model prediction to flight measurements: accuracy less than 15 % for GCR dose rates; ~25% for secondary particles ; and $\pm$30% for quality factors by TEPC.
  - Minor scientific questions remained: low-energy light ion cross section, albedo protons, secondary pions, and kaons.
- Space Radiation Shield Design Tool for the reliable and realistic radiation simulation in the early design process of exploration missions:
  - Environmental models, shielding and body geometry models, atomic and nuclear interaction and fragmentation models are incorporated.